Available online at http://scik.org
J. Math. Comput. Sci. 2024, 14:17
https://doi.org/10.28919/jmcs/7582
ISSN: 1927-5307

ANALYZING THE ROLE OF COMORBIDITY ON COVID-19 INFECTIONS BY MATHEMATICAL MODELING

MUSYOKA KINYILI[1,2,*], JEAN MS LUBUMA[2], JUSTIN B. MUNYAKAZI[3], ABDULAZIZ Y. A. MUKHTAR[3]

[1]Department of Mathematics and Statistics, University of Embu, P. O. Box 6-60100 Embu, Kenya

[2]School of Computer Science and Applied Mathematics, University of the Witwatersrand, Private Bag 3, Wits 2050, Johannesburg, South Africa

[3]Department of Mathematics and Applied Mathematics, Faculty of Natural Sciences, University of the Western Cape, Private Bag X17 Bellville 7535, South Africa

Abstract. This study develops a deterministic mathematical model to quantify the role played by comorbidity among humans as a risk factor for driving COVID-19 epidemic. The newly developed model is confined to those comorbidities that are not infectious and thus there is no transmission of comorbidities among individuals within the compartments of the model. Firstly, we carry out the quantitative and qualitative analysis of the model appertaining positivity, boundedness, equilibrium points, reproduction number, stability of the equilibrium points and bifurcation analysis. Secondly, we fit the model to real COVID-19 data of the Republic of South Africa to assure the validity of the model. Finally, we compute sensitivity indices with respect to the parameters of interest for the purpose of sensitivity interpretation and perform numerical simulations to assess the trajectory of COVID-19 infections as the parameters of interest vary. Results indicate that comorbidity contributes significantly in increasing the number of the COVID-19 infections.

Keywords: mathematical modeling; COVID-19 epidemic; deterministic models; comorbidity; reproduction number.

*Corresponding author

E-mail address: davismusyooo@gmail.com

Received February 02, 2024

2020 AMS Subject Classification: 92D30.

1. INTRODUCTION

It has been more that three years since the first case of COVID-19, the most recent coronavirus to be observed in humans was reported [1]–[3]. As indicated in [2],[4]–[8], its causative agent is the Severe Acute Respiratory Syndrome-Corona-Virus-2 (SARS-CoV-2). It has proved to be the most devastating coronavirus with its severity and rapidly spreading feature [9]. The disease was firstly reported in December 2019 at Wuhan, Hubei province in China [8],[10]–[12]. Since then, many countries globally have battled the epidemic. At least four variants of SARS-CoV-2 namely, α, β, γ and δ were experienced world-wide [13]. The disease infected millions of people as well as claiming millions of lives globally. To be more precise, as of April 4, 2022 (12:30 GMT), the world had recorded $491,930,645$ COVID-19 positive cases with 6,176,813 deaths. The Republic of South Africa alone had confirmed $3,722,954$ COVID-19 positive cases with 100,050 fatalities [14].

Data-based studies such as studies in [15, 16] have identified common comorbidities as hypertension, diabetes, cardiovascular disease, cerebrovascular disease, obesity, malignancy, liver disease, renal disease and Tuberculosis. Most of these comorbidities are also common in the Republic of South Africa which was the leading COVID-19 epicenter in Africa. A study in [17] on the relationship of COVID-19 and comorbidity showed that COVID-19 patients with comorbidity had worse clinical outcomes as compared to those without comorbidity. It further indicated that the higher the number of comorbidities, the greater the risk of serious adverse outcomes. More data-based studies on the relationship between COVID-19 and comorbidity are done in [18]–[23].

On the pathway of mathematical modeling, many studies have been done on the dynamics of the COVID-19. In particular, modeling studies done in [1, 2, 6],[24]–[33] have focused on the impacts of non-pharmaceutical control measures such as wearing of face masks, social distancing, lock-downs, quarantine, use of digital apps and hygienic practices. Other modeling studies such as studies done in [9],[34]–[41] have specialized on the impact assessment of vaccination against the COVID-19. However, few modeling studies have explored the relationship between COVID-19 and comorbidities. For instance, the study in [42] uses mathematical modelling to

analyze the co-existence of Diabetes and COVID-19. Another study in [43] devises a mathematical model of COVID-19 with comorbidity and controlling using non-pharmaceutical interventions and vaccination. The study in [44] models the COVID-19 pandemic and highlights the negative impact of quarantine on Diabetic people. Finally, a study in [13] uses mathematical modeling to analyze Tuberculosis and COVID-19 co-infection.

The present study seeks to develop a mathematical model that incorporates comorbidity as a risk driver of COVID-19. The model is confined particularly to those comorbidities that are not infectious thus they cannot be transmitted from one individual to another within the compartments of the model.

The rest of the paper is arranged as follows: In Section 2, we develop the model. Section 3 presents the quantitative and qualitative analysis of the system appertaining positivity, boundedness, equilibrium points, reproduction number, stability of the system equilibria and bifurcation. Section 4 presents numerical analysis of the model including model parameterization, sensitivity analysis, and simulations. Finally, Section 5 gives the conclusion.

2. MODEL DEVELOPMENT

Aiming to investigate the role of comorbidity on the transmission dynamics of the COVID-19 epidemic, we extend the standard *SEIR* mathematical model by introducing comorbidity in the susceptible population. The new mathematical model contains six compartments that is, susceptible individuals without comorbidity (S), susceptible individuals with comorbidity (S_c), exposed individuals (E), infectious individuals without comorbidity (I_0), infectious individuals with comorbidity (I_c) and the removed individuals from the chain of transmission of the COVID-19. The removed class here collects individuals who recover and those who die from the COVID-19. Thus the total population is assumed to be given by

$$N = S + S_c + E + I_0 + I_c + R. \tag{1}$$

We assume human to human transmission of the COVID-19, no transmission of the comorbidities within the classes of the model, all the compartments are mutually exclusive and individuals with comorbidity are highly vulnerable to the COVID-19 when exposed. The model generates

the following system of nonlinear ordinary differential equations

$$\frac{dS}{dt} = (1-\omega)\pi - (\lambda_s + \delta)S, \tag{2}$$

$$\frac{dS_c}{dt} = \omega\pi - (\lambda_c + \delta + \mu)S_c, \tag{3}$$

$$\frac{dE}{dt} = \lambda_s S + \lambda_c S_c - (\eta + \delta + \mu)E, \tag{4}$$

$$\frac{dI_0}{dt} = (1-\rho)\eta E - (\alpha + \delta)I_0, \tag{5}$$

$$\frac{dI_c}{dt} = \rho\eta E - (\psi + \delta + \mu)I_c, \tag{6}$$

$$\frac{dR}{dt} = \alpha I_0 + \psi I_c - (\delta + \mu)R. \tag{7}$$

We note that, just as many comorbidities have been, the COVID-19 has been endemic. Due to this reason, the model considers a recruitment rate of π where a proportion ω flux to the compartment of susceptible individuals with comorbidity S_c and the remaining proportion $(1-\omega)$ flux to the compartment of susceptible individuals without comorbidity S. Individuals with comorbidity progress to the exposed class E at the rate of β following close contact with COVID-19 infectious individuals. This defines the force of infection for the individuals with comorbidity denoted by λ_c on the model. Similarly, individuals without comorbidity move to the exposed class E at the rate of $\kappa\beta$ once they come into close contact with COVID-19 infectious individuals. Here, we confine $\kappa < 1$ since individuals with comorbidity are assumed to have a weaker immune system and thus are highly vulnerable to contraction of the COVID-19 infections than their counterparts. Thus, $\kappa\beta I$ defines the force of infection for the individuals without comorbidity represented by λ_s on the model. Therefore, the force of infection for the model is given by $\lambda_s + \lambda_c = (\kappa\beta + \beta)I$, where $I = I_0 + I_c$.

All the adequately exposed individuals collected in the latent class E progress to the COVID-19 infectious classes following completion of the incubation period η. A proportion ρ of the E class joins the class of the COVID-19 infectious individuals with comorbidity I_c whereas the remaining proportion $(1-\rho)$ flux to the COVID-19 infectious individuals without comorbidity I_0. Individuals with comorbidity get removed from the COVID-19 chain of transmission by recovery or death due to COVID-19 at the rate of ψ. Similarly, Individuals without comorbidity

move to the class of removed individuals R at the rate of α. Individuals from all the compartments of the model die naturally at the rate of δ whereas individuals in the S_c, E, I_c and R compartments additionally die due to comorbidity at the rate of μ. The schematic diagram for the model is represented by **Figure 1** with the parameters described in **Table 1**.

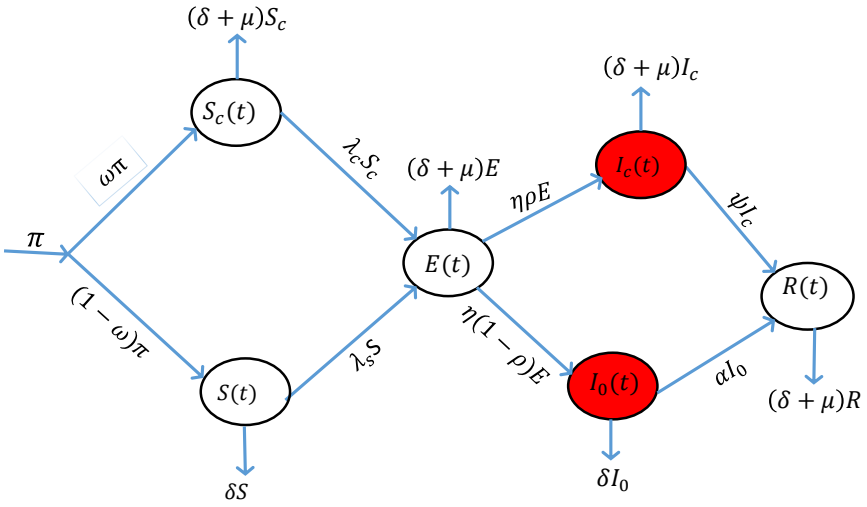

FIGURE 1. Schematic representation of the proposed model.

TABLE 1. Parameter description for the model (2)–(7) and their estimated values.

Symbol	Parameter Description	Value per day	Source
π	Rate of recruitment	11244	[24]
ω	Proportion of recruited individuals with comorbidity	0.2	Fitted
β	Rate of contact with COVID-19 infectious individuals	(0,2)	Variable
κ	Modification parameter for COVID-19 infection on individuals without comorbidity	0.2735	Fitted
ρ	Proportion of COVID-19 infectious individuals with comorbidity	(0,1)	Variable
η	Incubation period for COVID-19	0.1961	[36, 37]
ψ	Rate of recovery and/or death due to COVID-19 by infectious individuals with comorbidity	0.4217	Fitted
α	Rate of recovery and/or death due to COVID-19 by infectious individuals without comorbidity	0.0316	Fitted
μ	Rate of death due to comorbidity	0.0018	Fitted
δ	Rate of natural death	0.0001	[27]

3. Quantitative and Qualitative Analysis of the System

3.1. Positivity of the Solution. *Lemma 3.1:*

Suppose $S(0) \geq 0$, $S_c(0) \geq 0$, $E(0) \geq 0$, $I_0(0) \geq 0$, $I_c(0) \geq 0$, and $R(0) \geq 0$. Then $S(t)$, $S_c(t)$, $E(t)$, $I_0(t)$, $I_c(t)$ and $R(t)$ are positive $\forall\, t \geq 0$.

Proof

We solve equation (2) by integration using integrating factor $\exp\left\{\delta t + \int_0^t \kappa\beta I(\tau)d\tau\right\}$ such that we have

$$\frac{dS(t)}{dt}\exp\left\{\delta t + \int_0^t \kappa\beta I(\tau)d\tau\right\} + (\kappa\beta I(t) + \delta)S(t)\exp\left\{\delta t + \int_0^t \kappa\beta I(\tau)d\tau\right\}$$
$$= (1-\omega)\pi\exp\left\{\delta t + \int_0^t \kappa\beta I(\tau)d\tau\right\},$$
$$\frac{\left(dS(t)\exp\left\{\delta t + \int_0^t \kappa\beta I(\tau)d\tau\right\}\right)}{dt} = (1-\omega)\pi\exp\left\{\delta t + \int_0^t \kappa\beta I(\tau)d\tau\right\},$$
$$S(t)\exp\left\{\delta t + \int_0^t \kappa\beta I(\tau)d\tau\right\} - S(0) = \int_0^t (1-\omega)\pi\exp\left\{\delta t + \int_0^t \kappa\beta I(\tau)d\tau\right\}dt,$$
$$S(t) = S(0)\exp\left\{-\delta t - \int_0^t \kappa\beta I(\tau)d\tau\right\} + \exp\left\{-\delta t - \int_0^t \kappa\beta I(\tau)d\tau\right\}$$
$$\int_0^t (1-\omega)\pi\exp\left\{\delta t + \int_0^t \kappa\beta I(\tau)d\tau\right\}dt \geq 0.$$

This illustration shows that $S(t)$ is positive. Following the same procedure, similar expressions for $S_c(t)$, $E(t)$, $I_0(t)$, $I_c(t)$ and $R(t)$ of the system (2)–(7) can be obtained respectively as

$$S_c(t) = S_c(0)\exp\left\{-(\delta+\mu)(t) - \int_0^t \beta I(\tau)d\tau\right\} +$$
$$\exp\left\{-(\delta+\mu)(t) - \int_0^t \beta I(\tau)d\tau\right\}\int_0^t \omega\pi\exp\left\{(\delta+\mu)(t) + \int_0^t \beta I(\tau)d\tau\right\}dt \geq 0;$$
$$E(t) = E(0)\exp\{-(\eta+\delta+\mu)(t)\} + \exp\{-(\eta+\delta+\mu)(t)\}\int_0^t [(1-\omega)\pi S(t) + \omega\pi S_c(t)]$$
$$\exp\{(\eta+\delta+\mu)(t)\}\,dt \geq 0;$$
$$I_0(t) = I_0(0)\exp\{-(\alpha+\delta)(t)\} + \exp\{-(\alpha+\delta)(t)\}\int_0^t (1-\rho)\eta E(t)\exp\{(\alpha+\delta)(t)\}\,dt \geq 0;$$
$$I_c(t) = I_c(0)\exp\{-(\psi+\delta+\mu)(t)\} + \exp\{-(\psi+\delta+\mu)(t)\}\int_0^t \rho\eta E(t)\exp\{(\psi+\delta+\mu)(t)\}\,dt \geq 0;$$
$$R(t) = R(0)\exp\{-(\delta+\mu)(t)\} + \exp\{-(\delta+\mu)(t)\}\int_0^t [\alpha I_0(t) + \psi I_c(t)]\exp\{(\delta+\mu)(t)\}\,dt \geq 0.$$

This proves that $S_c(t)$, $E(t)$, $I_0(t)$, $I_c(t)$ and $R(t)$ are also positive hence the solution of the model (2)–(7) is positive $\forall\, t \geq 0$.

3.2. Boundedness of the Model.

Lemma 3.2: Let $\Lambda_{\mathscr{R}} = \left\{(S, S_c, E, I_0, I_c, R) \in \mathbb{R}^6_+ : S + S_c + E + I_0 + I_c + R \leq \frac{\pi}{\delta}\right\}$ denote a uniformly bounded region defined for all $t \geq 0$. Then, $\Lambda_{\mathscr{R}}$ is positively invariant and attracting with respect to the model (2)–(7) and the model can be considered as epidemiologically and mathematically well posed within the region.

Proof

Adding all the equations of the model (2)–(7), we obtain

$$\begin{aligned} \frac{dN}{dt} &= \pi - \delta N - \mu(S_c + E + I_c + R) \\ &\leq \pi - \delta N. \end{aligned} \tag{8}$$

Solving (8) by applying integration factor and the Gronwall Inequality with $N(0) = N_0$ yields

$$N(t) \leq \frac{\pi}{\delta}\left(1 - e^{-\delta t}\right) + N_0 e^{-\delta t}. \tag{9}$$

It thus follows that

$$\lim_{t\to\infty} \sup\{N(t)\} \leq \frac{\pi}{\delta}. \tag{10}$$

From (10) we see that $N \leq \frac{\pi}{\delta}$, $\forall t \geq 0$. This proves that N is bounded and thus the biological feasible region $\Lambda_{\mathscr{R}}$ is positively invariant and attracting for all $t \geq 0$. Hence, the solution of the model is confined within the defined region.

3.3. The System Equilibria.

We determine the equilibrium points of the model system (2)–(7) at the steady state. We do so by first setting the left hand side of the system (2)–(7) to zero. We noted that, solving the system explicitly at the steady state is cumbersome and not straight forward. Thus, we solve the system in terms of forces of infections λ_s and λ_c at the steady state as

$$\begin{aligned} S^* &= \frac{(1-\omega)\pi}{\lambda_s + \delta}, \\ S_c^* &= \frac{\pi\omega}{(\lambda_c + \delta + \mu)}, \end{aligned}$$

$$
\begin{aligned}
E^* &= \frac{\lambda_s(1-\omega)(\lambda_c+\delta+\mu)\pi+\lambda_c\pi\omega(\lambda_s+\delta)}{(\lambda_s+\delta)(\lambda_c+\delta+\mu)(\eta+\delta+\mu)},\\
I_0^* &= \frac{(1-\rho)\eta}{\alpha+\delta}\left(\frac{\lambda_s(1-\omega)(\lambda_c+\delta+\mu)\pi+\lambda_c\pi\omega(\lambda_s+\delta)}{(\lambda_s+\delta)(\lambda_c+\delta+\mu)(\eta+\delta+\mu)}\right), \qquad (11)\\
I_c^* &= \frac{\rho\eta}{\psi+\delta+\mu}\left(\frac{\lambda_s(1-\omega)(\lambda_c+\delta+\mu)\pi+\lambda_c\pi\omega(\lambda_s+\delta)}{(\lambda_s+\delta)(\lambda_c+\delta+\mu)(\eta+\delta+\mu)}\right),\\
R^* &= \left(\frac{\rho\eta}{\psi+\delta+\mu}+\frac{(1-\rho)\eta}{\alpha+\delta}\right)\left(\frac{\lambda_s(1-\omega)(\lambda_c+\delta+\mu)\pi+\lambda_c\pi\omega(\lambda_s+\delta)}{(\lambda_s+\delta)(\lambda_c+\delta+\mu)(\eta+\delta+\mu)}\right).
\end{aligned}
$$

If $\lambda_s = 0$ and $\lambda_c = 0$ on the system (11), then we obtain the disease free equilibrium point given by

$$
\mathscr{E}^0 = \left(\frac{(1-\omega)\pi}{\delta}, \frac{\omega\pi}{\delta+\mu}, 0, 0, 0, 0\right). \qquad (12)
$$

This means that, since the force of infections is zero, then it implies that there are no infectious individuals in the population of concern. This instance is referred to as the disease free equilibrium [27, 45].

If $\lambda_s \neq 0$ and $\lambda_c \neq 0$ then this defines a situation when the endemic equilibrium point of the model exists. We determine the conditions for existence of the endemic equilibrium point of the model later in **Section 3.5**.

3.4. Basic Reproduction Number. We employ the next generation operator technique to compute the basic reproduction number $\mathscr{R}_0$ [9, 45]. The $\mathscr{R}_0$ here represents the secondary number of infections caused by a single infectious individual when introduced into a susceptible population [27]. From the model system (2)–(7), the classes which are involved in the spread of the COVID-19 epidemic are $E(t)$, $I_0(t)$ and $I_c(t)$. Therefore we can write the system (2)–(7) into the reduced form as

$$
\begin{aligned}
\frac{dE}{dt} &= \kappa\beta IS + \beta IS_c - (\eta+\delta+\mu)E,\\
\frac{dI_0}{dt} &= (1-\rho)\eta E - (\alpha+\delta)I_0, \qquad (13)\\
\frac{dI_c}{dt} &= \rho\eta E - (\psi+\delta+\mu)I_c.
\end{aligned}
$$

We re-write the system (13) in compact matrix form separating the linear and the non-linear parts as

$$\frac{d\mathbf{X}}{dt} = \mathscr{F}(\mathbf{X}) - \mathscr{V}(\mathbf{X}), \tag{14}$$

where $\mathbf{X} = [E, I_0, I_c]^T$,

$$\mathscr{F} = \begin{pmatrix} \kappa\beta IS + \beta IS_c \\ 0 \\ 0 \end{pmatrix}, \tag{15}$$

and

$$\mathscr{V} = \begin{pmatrix} (\eta+\delta+\mu)E \\ -(1-\rho)\eta E + (\alpha+\delta)I_0 \\ -\rho\eta E + (\psi+\delta+\mu)I_c \end{pmatrix}. \tag{16}$$

In epidemiological terms, the matrix $\mathscr{F}$ denotes the new infections whereas $\mathscr{V}$ is the transfer of infections within the compartments. The transition matrices F and V are obtained respectively as the Jacobian of $\mathscr{F}$ and $\mathscr{V}$ with respect to E, I_0 and I_c, evaluated at the disease free equilibrium $\mathscr{E}^0 = \left(\frac{(1-\omega)\pi}{\delta}, \frac{\omega\pi}{\delta+\mu}, 0, 0, 0, 0\right)$ as

$$F = \begin{pmatrix} 0 & \frac{\kappa\beta(1-\omega)\pi}{\delta} & \frac{\beta\omega\pi}{\delta+\mu} \\ 0 & 0 & 0 \\ 0 & 0 & 0 \end{pmatrix}, \tag{17}$$

and

$$V = \begin{pmatrix} \eta+\delta+\mu & 0 & 0 \\ -(1-\rho)\eta & \alpha+\delta & 0 \\ -\rho\eta & 0 & \psi+\delta+\mu \end{pmatrix}. \tag{18}$$

The next generation matrix is defined by FV^{-1}, where the reproduction number is the dominant eigenvalue of the matrix FV^{-1}. We now have

$$FV^{-1} = \begin{pmatrix} \left\{\frac{\rho\eta}{(\eta+\delta+\mu)(\psi+\delta+\mu)} + \frac{(1-\rho)\eta}{(\eta+\delta+\mu)(\alpha+\delta)}\right\}\mathscr{P} & \frac{\mathscr{P}}{\alpha+\delta} & \frac{\mathscr{P}}{\psi+\delta+\mu} \\ 0 & 0 & 0 \\ 0 & 0 & 0 \end{pmatrix} \tag{19}$$

where

$$\mathscr{P} = \beta\pi\left(\frac{(1-\omega)\kappa}{\delta}+\frac{\omega}{\delta+\mu}\right).$$

Hence, the basic reproduction number of the model is

$$\mathscr{R}_0 = \beta\pi\left(\frac{(1-\omega)\kappa}{\delta}+\frac{\omega}{\delta+\mu}\right)\left\{\frac{\rho\eta}{(\eta+\delta+\mu)(\psi+\delta+\mu)}+\frac{(1-\rho)\eta}{(\eta+\delta+\mu)(\alpha+\delta)}\right\}. \tag{20}$$

3.5. Existence of Endemic Equilibrium Point. We determine the conditions for existence of the endemic equilibrium point (EEP) of the model. This is done by substituting (11) into $\lambda_c^* = \beta(I_0^*+I_c^*)$ with $\lambda_s^* = \kappa\lambda_c^*$ and solving the the force of infections equation when $\lambda_c = \lambda_c^* \neq 0$ as follows

$$\lambda_c^* = \left(\frac{\beta\rho\eta}{\psi+\delta+\mu}+\frac{\beta(1-\rho)\eta}{\alpha+\delta}\right)\left(\frac{\kappa\lambda_c^*(1-\omega)(\lambda_c^*+\delta+\mu)\pi+\lambda_c^*\pi\omega(\kappa\lambda_c^*+\delta)}{(\kappa\lambda_c^*+\delta)(\lambda_c^*+\delta+\mu)(\eta+\delta+\mu)}\right). \tag{21}$$

Rearranging equation (21) and factoring out λ_c^* we have

$$\lambda_c^*(\kappa\lambda_c^*+\delta)(\lambda_c^*+\delta+\mu)(\eta+\delta+\mu)-\lambda_c^*(\kappa(1-\omega)\pi(\lambda_c^*+\delta+\mu)+(\kappa\lambda_c^*+\delta)\pi\omega) \left(\frac{\beta\rho\eta}{\psi+\delta+\mu}+\frac{\beta(1-\rho)\eta}{\alpha+\delta}\right)=0. \tag{22}$$

From (22), we claim that if $\lambda_c^* \neq 0$, then

$$(\kappa\lambda_c^*+\delta)(\lambda_c^*+\delta+\mu)(\eta+\delta+\mu)-(\kappa(1-\omega)\pi(\lambda_c^*+\delta+\mu)+(\kappa\lambda_c^*+\delta)\pi\omega) \left(\frac{\beta\rho\eta}{\psi+\delta+\mu}+\frac{\beta(1-\rho)\eta}{\alpha+\delta}\right)=0. \tag{23}$$

Expanding (23) and collecting like terms together we obtain a quadratic equation as

$$P_2(\lambda_c^*)^2+P_1\lambda_c^*+P_0=0 \tag{24}$$

where

$$P_2=\kappa, P_0=(1-\mathscr{R}_0)(\delta+\mu)\delta,$$
$$P_1=(\delta+\mu)\kappa+\delta-\frac{\kappa\pi}{\eta+\delta+\mu}\left(\frac{\beta\rho\eta}{\psi+\delta+\mu}+\frac{\beta(1-\rho)\eta}{\alpha+\delta}\right). \tag{25}$$

The solution of (24) is given as

$$\lambda_c^* = \frac{-P_1 \pm \sqrt{P_1^2 - 4P_2P_0}}{2P_2}. \tag{26}$$

From (26), we claim that the model (2)–(7) has

(i) *a unique endemic equilibrium if* $P_1^2 - 4P_2P_0 = 0$;

(ii) *two endemic equilibria if* $P_0 < 0$ *or* $P_1^2 - 4P_2P_0 > 0$;

(iii) *no endemic equilibrium otherwise*.

Here, we note that the disease EEP exists when $\mathscr{R}_0 > 1$ [45] and thus Case (ii) is the only case that guarantees the existence of at least one positive EEP for the model (2)–(7). Since it is biologically sound that the EEP must be positive, then based on the Case (ii), we further give conditions for existence of at least one positive EEP for the model as follows

(a) *one unique positive endemic equilibrium if* $P_1 < 0$ *and* $P_1 < \sqrt{P_1^2 - 4P_2P_0}$ *or,* $P_1 > 0$ *and* $P_1 < \sqrt{P_1^2 - 4P_2P_0}$;

(b) *two positive endemic equilibria if* $P_1 < 0$ *and* $P_1 > \sqrt{P_1^2 - 4P_2P_0}$;

(c) *no positive endemic equilibrium otherwise*.

Furthermore, holding the Case (ii) true, we give more narrowed conditions for the existence of a positive EEP of the model based on the Descartes' rule of sign changes. Thus, examining the signs of the coefficients of (24), it is clear from (25) that $P_2 > 0$ and $P_0 < 0$ if and only if $\mathscr{R}_0 > 1$. However, the sign of P_1 is not clear. Therefore, we summarize the conditions for existence of positive endemic equilibrium point(s) of the model in **Table 2**.

TABLE 2. Existence of positive endemic equilibrium of the model (2)–(7) .

Case	**Sign of P_2**	**Sign of P_1**	**Sign of P_0**	**No. of Sign Changes**	**Conclusion**
1	+	+	−	1	*a unique endemic equilibrium*
2	+	−	−	1	*a unique endemic equilibrium*

Based on the results in **Table 2**, it is clear that model (2)–(7) has a unique endemic equilibrium point.

3.6. Local Stability of the System Equilibria. We discuss the local asymptomatic stability criteria of the equilibrium points of the model (2)–(7) by evaluating the Jacobian and the resulting characteristic equations. We then scrutinize the signs of the eigenvalues based on the Routh–Hurwitz conditions. The Jacobian of the model system (2)–(7) is given by

$$J = \begin{pmatrix} -\kappa\beta I-\delta & 0 & 0 & -\kappa\beta S & -\kappa\beta S & 0 \\ 0 & -\beta I-\delta-\mu & 0 & -\beta S_c & -\beta S_c & 0 \\ \kappa\beta I & \beta I & -(\eta+\delta+\mu) & \kappa\beta S+\beta S_c & \kappa\beta S+\beta S_c & 0 \\ 0 & 0 & (1-\rho)\eta & -(\alpha+\delta) & 0 & 0 \\ 0 & 0 & \rho\eta & 0 & -(\psi+\delta+\mu) & 0 \\ 0 & 0 & 0 & \alpha & \psi & -(\delta+\mu) \end{pmatrix}. \tag{27}$$

Lemma 3.6:

The disease free equilibrium $\mathscr{E}^0 = \left(\frac{(1-\omega)\pi}{\delta}, \frac{\omega\pi}{\delta+\mu}, 0, 0, 0, 0\right)$ is locally asymptotically stable if $\mathscr{R}_0 < 1$ and unstable if $\mathscr{R}_0 > 1$.

Proof

The Jacobian matrix given by equation (27) evaluated at the disease free equilibrium is obtained as

$$J(\mathscr{E}^0) = \begin{pmatrix} -\delta & 0 & 0 & -\kappa\beta S^0 & -\kappa\beta S^0 & 0 \\ 0 & -\delta-\mu & 0 & -\beta S_c^0 & -\beta S_c^0 & 0 \\ 0 & 0 & -(\eta+\delta+\mu) & \kappa\beta S^0+\beta S_c^0 & \kappa\beta S^0+\beta S_c^0 & 0 \\ 0 & 0 & (1-\rho)\eta & -(\alpha+\delta) & 0 & 0 \\ 0 & 0 & \rho\eta & 0 & -(\psi+\delta+\mu) & 0 \\ 0 & 0 & 0 & \alpha & \psi & -(\delta+\mu) \end{pmatrix}. \tag{28}$$

Using equation (28), we obtain the characteristic equation as

$$(-\delta-\lambda)(-\delta-\mu-\lambda)(-\delta-\mu-\lambda)(a_3\lambda^3+a_2\lambda^2+a_1\lambda+a_0) = 0 \tag{29}$$

where

$$a_3 = 1, a_2 = \eta + 3\delta + 2\mu + \alpha + \psi, a_0 = (1-\mathscr{R}_0)(\eta+\delta+\mu)(\alpha+\delta)(\psi+\delta+\mu)$$
$$a_1 = (\alpha+2\delta+\psi+\mu)(\eta+\delta+\mu)+(\alpha+\delta)(\psi+\delta+\mu)-\eta\beta\pi\left(\frac{(1-\omega)\kappa}{\delta}+\frac{\omega}{\delta+\mu}\right).$$

(30)

It is clear from equation (29) that the first three eigenvalues are negative real values and the rest of the eigenvalues can be obtained by solving the cubic polynomial $a_3\lambda^3 + a_2\lambda^2 + a_1\lambda + a_0 = 0$. Applying the Routh–Hurwitz criterion on the cubic polynomials, it requires that $a_3 > 0$, $a_2 > 0$, $a_0 > 0$ and $a_2a_1 - a_3a_0 > 0$, for the remaining three eigenvalues to be negative or have negative real parts. Clearly from (30), $a_3 > 0$, $a_2 > 0$, $a_0 > 0$ if and only if $\mathscr{R}_0 < 1$ and $a_2a_1 > a_3a_0$ if and only if $\mathscr{R}_0 < 1$. This satisfies the Routh–Hurwitz conditions for a cubic polynomial if $\mathscr{R}_0 < 1$ and hence the disease free equilibrium is locally asymptotically stable.

For the Jacobian matrix evaluated at the disease endemic equilibrium point we have

$$J(\mathscr{E}^*) = \begin{pmatrix} -(\kappa\beta I^*+\delta) & 0 & 0 & -\kappa\beta S^* & -\kappa\beta S^* & 0 \\ 0 & -(\beta I^*+\delta+\mu) & 0 & -\beta S_c^* & -\beta S_c^* & 0 \\ \kappa\beta I^* & \beta I^* & -(\eta+\delta+\mu) & \kappa\beta S^*+\beta S_c^* & \kappa\beta S^*+\beta S_c^* & 0 \\ 0 & 0 & (1-\rho)\eta & -(\alpha+\delta) & 0 & 0 \\ 0 & 0 & \rho\eta & 0 & -(\psi+\delta+\mu) & 0 \\ 0 & 0 & 0 & \alpha & \psi & -(\delta+\mu) \end{pmatrix}. \tag{31}$$

For convenience, let us denote $B_1 = \kappa\beta I^* + \delta$, $B_2 = \beta I^* + \delta + \mu$, $B_3 = \eta + \delta + \mu$, $B_4 = \alpha + \delta$, $B_5 = \psi + \delta + \mu$, $M = \kappa\beta S^*$, $N = \beta S_c^*$ and $A = M + N$. Then from equation (31), the characteristic equation is

$$(-\delta-\mu-\lambda)(a_5\lambda^5 + a_4\lambda^4 + a_3\lambda^3 + a_2\lambda^2 + a_1\lambda + a_0) = 0 \tag{32}$$

where,

$$a_5 = 1, a_4 = B_5 + B_4 + B_3 + B_2 + B_1,$$
$$a_3 = B_4B_5 + B_3B_5 + B_1B_5 + B_2B_5 + B_3B_4 + B_1B_4 + B_2B_4 + B_1B_3 + B_2B_3 + B_1B_2 - \rho\eta A,$$
$$a_2 = B_3B_4B_5 + B_1B_4B_5 + B_2B_4B_5 + B_1B_3B_5 + B_2B_3B_5 + B_1B_3B_5 + B_1B_2B_5 + B_1B_3B_4$$

$$+B_2B_3B_4+B_1B_2B_4+B_1B_2B_3+(M+N)\rho\eta-(B_4+B_2+B_1)\rho\eta A-(B_5+B_2+B_1)(1-\rho)\eta A,$$

$$a_1=B_1B_3B_4B_5+B_2B_3B_4B_5+B_1B_2B_4B_5+B_1B_2B_3B_5+B_1B_3B_4B_4+(B_1+B_4)\rho\eta N^2$$
$$+(B_1+B_5)(1-\rho)\eta N^2+(B_2+B_4)\rho\eta M^2+(B_2+B_5)(1-\rho)\eta M^2$$
$$-(B_1B_4+B_2B_4+B_1B_2)\rho\eta A-(B_1B_5+B_2B_5+B_1B_2)(1-\rho)\eta A,$$

$$a_0=B_1B_2B_3B_4B_5+B_1B_4\rho\eta N^2+B_1B_5(1-\rho)\eta N^2+B_2B_4\rho\eta M^2+B_2B_5(1-\rho)\eta M^2$$
$$-B_1B_2B_4\rho\eta A-B_1B_2B_5(1-\rho)\eta A.$$

From equation (32), we see that the first eigenvalue is a negative real value and the other eigenvalues can be obtained by solving the fifth-ordered polynomial $a_5\lambda^5+a_4\lambda^4+a_3\lambda^3+a_2\lambda^2+a_1\lambda+a_0=0$. By the Routh–Hurwitz criterion on the fifth-ordered polynomials, the following conditions need to be satisfied for the remaining five eigenvalues to be negative or have negative real parts: $a_5>0$, $a_4>0$, $a_0>0$, $a_4a_3-a_5a_2>0$, $a_3a_4a_2+a_4a_5a_0-a_5a_2^2-a_1a_4^2>0$ and $a_4a_1-a_5a_0-(a_4a_3-a_5a_2)^2a_0>0$. Thus the disease endemic equilibrium point of the model is stable if the above conditions are satisfied and unstable otherwise. This is not very clear and thus the bifurcation of the model is discussed later in **Section 3.8**.

3.7. Global Stability of the Disease Free Equilibrium. To determine the global stability of the model's disease free equilibrium, we need to express the system (2)–(7) in the form, $\frac{d\mathbf{P}}{dt}=Y(\mathbf{P},\mathbf{Q})$, $\frac{d\mathbf{Q}}{dt}=M(\mathbf{P},\mathbf{Q})$, $M(\mathbf{P},0)=0$, where $\mathbf{P}$ denotes the collection of non-disease classes and $\mathbf{Q}$ represents the collection of disease classes of the model, and show that the following conditions hold whenever $\mathscr{R}_0<1$

$C_1:$ $\frac{d\mathbf{P}}{dt}=Y(\mathbf{P},0)$, $\mathbf{P}^0$ is globally asymptotically stable.

$C_2:$ $M(\mathbf{P},\mathbf{Q})=N\mathbf{Q}-\widetilde{M}(\mathbf{P},\mathbf{Q})$, $\widetilde{M}(\mathbf{P},\mathbf{Q})\geq 0$ for $(\mathbf{P},\mathbf{Q})\in\mathbb{R}^6_+$ where $N=\frac{\partial M}{\partial\mathbf{Q}}\mathscr{E}^0$ and $\mathbb{R}^6_+$ is the region where the model makes biological sense.

From the model system (2)–(7), we find that $\mathbf{P}=(S,S_c,R)^T$ and $\mathbf{Q}=(E,I_0,I_c)^T$. The disease free equilibrium of the model is $\mathscr{E}^0=(\mathbf{P}^0,0)=\left(\frac{(1-\omega)\pi}{\delta},\frac{\omega\pi}{\delta+\mu},0,0,0,0\right)$. The point $\mathscr{E}^0=(\mathbf{P}^0,0)$ is globally asymptotically stable if $\mathscr{R}_0<1$, hence

$$\frac{d\mathbf{P}}{dt} = Y(\mathbf{P},0) = \begin{bmatrix} (1-\omega)\pi - \delta S \\ \omega\pi - (\delta+\mu)S_c \\ 0 \\ 0 \end{bmatrix},$$

and thus C_1 is satisfied. We then check the satisfaction of C_2 as

$$N\mathbf{Q} = \begin{pmatrix} -(\eta+\delta+\mu) & 0 & 0 \\ (1-\rho)\eta & -(\alpha+\delta) & 0 \\ \rho\eta & 0 & -(\psi+\delta+\mu) \end{pmatrix} \begin{pmatrix} E \\ I_0 \\ I_c \end{pmatrix}$$

and

$$M(\mathbf{P},\mathbf{Q}) = \begin{pmatrix} \kappa\beta(I_0+I_c)S + \beta(I_0+I_c)S_c \\ (1-\rho)\eta E - (\alpha+\delta)I_0 \\ \rho\eta E - (\psi+\delta+\mu)I_c \end{pmatrix}.$$

Using $M(\mathbf{P},\mathbf{Q}) = N\mathbf{Q} - \widetilde{M}(\mathbf{P},\mathbf{Q})$ then,

$$\widetilde{M}(\mathbf{P},\mathbf{Q}) = \begin{pmatrix} \kappa\beta(I_0+I_c)\left(1-\frac{S}{N}\right) + \beta(I_0+I_c)\left(1-\frac{S_c}{N}\right) \\ 0 \\ 0 \end{pmatrix}.$$

hence $\widetilde{M}(\mathbf{P},\mathbf{Q}) \geq 0$ since $\frac{S}{N} \leq 1$ and $\frac{S_c}{N} \leq 1$. Thus, C_2 is satisfied. This proves that the model's disease free equilibrium is globally asymptotically stable whenever $\mathscr{R}_0 < 1$.

3.8. Bifurcation analysis of the Model. We determine the nature of bifurcation of the model system (2)–(7) when $\mathscr{R}_0 = 1$. To achieve this, we adopt the Center Manifold Theory established in [46] and also applied in [13, 43, 47]. We choose the bifurcation parameter to be $\phi = \beta = \beta^*$, find the values of a and b given by (33)–(34) and assess their signs for the necessary conclusion.

$$a = \sum_{i,j,k=1}^{6} v_k w_i w_j \frac{\partial^2 f_k}{\partial x_i \partial x_j}(\mathscr{E}^0, \beta^*), \tag{33}$$

$$b = \sum_{i,k=1}^{6} v_k w_i \frac{\partial^2 f_k}{\partial x_i \partial \beta}(\mathscr{E}^0, \beta^*), \tag{34}$$

where w and v are respectively, the right and the left eigenvectors having zero eigenvalue to the Jacobian matrix of the system (2)–(7) evaluated at the disease free equilibrium $\mathscr{E}^0$ when $\beta = \beta^*$, f is the time derivatives of the state variables and x is the state variables; i, j, k are respectively the i^{th}, j^{th} and k^{th} components.

For the right eigenvector w_i given by $J(\mathscr{E}^0)(w_i)^T = 0$, we have

$$\begin{pmatrix} -\delta & 0 & 0 & -\kappa\beta S^0 & -\kappa\beta S^0 & 0 \\ 0 & -\delta-\mu & 0 & -\beta S_c^0 & -\beta S_c^0 & 0 \\ 0 & 0 & -(\eta+\delta+\mu) & \kappa\beta S^0+\beta S_c^0 & \kappa\beta S^0+\beta S_c^0 & 0 \\ 0 & 0 & (1-\rho)\eta & -(\alpha+\delta) & 0 & 0 \\ 0 & 0 & \rho\eta & 0 & -(\psi+\delta+\mu) & 0 \\ 0 & 0 & 0 & \alpha & \psi & -(\delta+\mu) \end{pmatrix} \begin{pmatrix} w_1 \\ w_2 \\ w_3 \\ w_4 \\ w_5 \\ w_6 \end{pmatrix} = \begin{pmatrix} 0 \\ 0 \\ 0 \\ 0 \\ 0 \\ 0 \end{pmatrix}. \tag{35}$$

From equation (35) we obtain

$$w_1 = -\frac{\kappa\beta S^0}{\delta}(w_4+w_5) < 0, w_2 = -\frac{\beta S_c^0}{\delta+\mu}(w_4+w_5) < 0, w_3 = \frac{\kappa\beta S^0+\beta S_c^0}{\eta+\delta+\mu}(w_4+w_5) > 0,$$
$$w_4 = \frac{(1-\rho)\eta}{\alpha+\delta}w_3 > 0, w_5 = \frac{\rho\eta}{\psi+\delta+\mu}w_3 > 0, w_6 = \frac{\alpha w_4+\psi w_5}{\delta+\mu} > 0. \tag{36}$$

For the left eigenvector v_i given by $(J(\mathscr{E}^0))^T(v_i)^T = 0$, we have

$$\begin{pmatrix} -\delta & 0 & 0 & 0 & 0 & 0 \\ 0 & -\delta-\mu & 0 & 0 & 0 & 0 \\ 0 & 0 & -(\eta+\delta+\mu) & (1-\rho)\eta & \rho\eta & 0 \\ -\kappa\beta S^0 & -\beta S_c^0 & \kappa\beta S^0+\beta S_c^0 & -(\alpha+\delta) & 0 & \alpha \\ -\kappa\beta S^0 & -\beta S_c^0 & \kappa\beta S^0+\beta S_c^0 & 0 & -(\psi+\delta+\mu) & \psi \\ 0 & 0 & 0 & 0 & 0 & -(\delta+\mu) \end{pmatrix} \begin{pmatrix} v_1 \\ v_2 \\ v_3 \\ v_4 \\ v_5 \\ v_6 \end{pmatrix} = \begin{pmatrix} 0 \\ 0 \\ 0 \\ 0 \\ 0 \\ 0 \end{pmatrix}. \tag{37}$$

From equation (37) we get

$$v_1 = v_2 = v_6 = 0,$$
$$v_3 = \frac{(1-\rho)\eta v_4+\rho\eta v_5}{\eta+\delta+\mu} > 0,$$

$$
\begin{aligned}
v_4 &= \frac{\kappa\beta S^0 + \beta S_c^0}{\alpha+\delta} v_3 > 0, \\
v_5 &= \frac{\kappa\beta S^0 + \beta S_c^0}{\psi+\delta+\mu} v_3 > 0.
\end{aligned} \tag{38}
$$

We next incorporate some change of symbols in the model (2)–(7) such that $S = x_1$; $S_c = x_2$; $E = x_3$; $I_0 = x_4$; $I_c = x_5$; $R = x_6$ and $\frac{dx_i}{dt} = f_i$, where $i = 1,2,3,4,5,6$. Thus, we have

$$
\begin{aligned}
\frac{dS}{dt} &:= f_1 = (1-\omega)\pi - \kappa\beta(x_4+x_5)x_1 - \delta x_1, \\
\frac{dS_c}{dt} &:= f_2 = \omega\pi - \beta(x_4+x_5)x_2 - (\delta+\mu)x_2, \\
\frac{dE}{dt} &:= f_3 = \kappa\beta(x_4+x_5)x_1 + \beta(x_4+x_5)x_2 - (\eta+\delta+\mu)x_3, \\
\frac{dI_0}{dt} &:= f_4 = (1-\rho)\eta x_3 - (\alpha+\delta)x_4, \\
\frac{dI_c}{dt} &:= f_5 = \rho\eta x_3 - (\psi+\delta+\mu)x_5, \\
\frac{dR}{dt} &:= f_6 = \alpha x_4 + \psi x_5 - (\delta+\mu)x_6.
\end{aligned} \tag{39}
$$

Using (39) we obtain

$$
\begin{aligned}
\frac{\partial^2 f_1}{\partial x_1 \partial x_4}(\mathscr{E}^0,\beta^*) = \frac{\partial^2 f_1}{\partial x_1 \partial x_5}(\mathscr{E}^0,\beta^*) = \frac{\partial^2 f_1}{\partial x_4 \partial x_1}(\mathscr{E}^0,\beta^*) = \frac{\partial^2 f_1}{\partial x_5 \partial x_1}(\mathscr{E}^0,\beta^*) = -\kappa\beta^*; \\
\frac{\partial^2 f_2}{\partial x_2 \partial x_4}(\mathscr{E}^0,\beta^*) = \frac{\partial^2 f_2}{\partial x_2 \partial x_5}(\mathscr{E}^0,\beta^*) = \frac{\partial^2 f_2}{\partial x_4 \partial x_2}(\mathscr{E}^0,\beta^*) = \frac{\partial^2 f_2}{\partial x_5 \partial x_2}(\mathscr{E}^0,\beta^*) = -\beta^*; \\
\frac{\partial^2 f_3}{\partial x_1 \partial x_4}(\mathscr{E}^0,\beta^*) = \frac{\partial^2 f_3}{\partial x_1 \partial x_5}(\mathscr{E}^0,\beta^*) = \frac{\partial^2 f_3}{\partial x_4 \partial x_1}(\mathscr{E}^0,\beta^*) = \frac{\partial^2 f_3}{\partial x_5 \partial x_1}(\mathscr{E}^0,\beta^*) = \kappa\beta^*; \\
\frac{\partial^2 f_3}{\partial x_2 \partial x_4}(\mathscr{E}^0,\beta^*) = \frac{\partial^2 f_3}{\partial x_2 \partial x_5}(\mathscr{E}^0,\beta^*) = \frac{\partial^2 f_3}{\partial x_4 \partial x_2}(\mathscr{E}^0,\beta^*) = \frac{\partial^2 f_3}{\partial x_5 \partial x_2}(\mathscr{E}^0,\beta^*) = \beta^*; \\
\frac{\partial^2 f_1}{\partial x_1 \partial x_j}(\mathscr{E}^0,\beta^*) = \frac{\partial^2 f_2}{\partial x_2 \partial x_j}(\mathscr{E}^0,\beta^*) = \frac{\partial^2 f_3}{\partial x_1 \partial x_j}(\mathscr{E}^0,\beta^*) = \frac{\partial^2 f_3}{\partial x_2 \partial x_j}(\mathscr{E}^0,\beta^*) = 0, \forall j = 1,2,3,6; \\
\frac{\partial^2 f_1}{\partial x_4 \partial x_j}(\mathscr{E}^0,\beta^*) = \frac{\partial^2 f_1}{\partial x_5 \partial x_j}(\mathscr{E}^0,\beta^*) = 0, \forall j = 2,3,4,5,6; \\
\frac{\partial^2 f_2}{\partial x_4 \partial x_j}(\mathscr{E}^0,\beta^*) = \frac{\partial^2 f_2}{\partial x_5 \partial x_j}(\mathscr{E}^0,\beta^*) = 0, \forall j = 1,3,4,5,6; \\
\frac{\partial^2 f_3}{\partial x_3 \partial x_j}(\mathscr{E}^0,\beta^*) = \frac{\partial^2 f_4}{\partial x_i \partial x_j}(\mathscr{E}^0,\beta^*) = \frac{\partial^2 f_5}{\partial x_i \partial x_j}(\mathscr{E}^0,\beta^*) = \frac{\partial^2 f_6}{\partial x_i \partial x_j}(\mathscr{E}^0,\beta^*) = 0, \forall i,j = 1,2,3,4,5,6; \\
\frac{\partial^2 f_3}{\partial x_4 \partial x_j}(\mathscr{E}^0,\beta^*) = \frac{\partial^2 f_3}{\partial x_5 \partial x_j}(\mathscr{E}^0,\beta^*) = 0, \forall j = 3,4,5,6.
\end{aligned} \tag{40}
$$

Similarly,

$$\frac{\partial^2 f_1}{\partial x_4 \partial \beta}(\mathscr{E}^0, \beta^*) = \frac{\partial^2 f_1}{\partial x_5 \partial \beta}(\mathscr{E}^0, \beta^*) = -\kappa x_1^0;$$
$$\frac{\partial^2 f_2}{\partial x_4 \partial \beta}(\mathscr{E}^0, \beta^*) = \frac{\partial^2 f_2}{\partial x_5 \partial \beta}(\mathscr{E}^0, \beta^*) = -x_2^0;$$
$$\frac{\partial^2 f_1}{\partial x_i \partial \beta}(\mathscr{E}^0, \beta^*) = \frac{\partial^2 f_2}{\partial x_i \partial \beta}(\mathscr{E}^0, \beta^*) = \frac{\partial^2 f_3}{\partial x_i \partial \beta}(\mathscr{E}^0, \beta^*) = 0, \forall i = 1,2,3,6; \tag{41}$$
$$\frac{\partial^2 f_3}{\partial x_4 \partial \beta}(\mathscr{E}^0, \beta^*) = \frac{\partial^2 f_3}{\partial x_5 \partial \beta}(\mathscr{E}^0, \beta^*) = \kappa x_1^0 + x_2^0;$$
$$\frac{\partial^2 f_k}{\partial x_i \partial \beta}(\mathscr{E}^0, \beta^*) = 0, \forall k = 4,5,6; i = 1,2,3,4,5,6.$$

Inserting (36), (38) and (40) in (33) we obtain the value of a as

$$a = (2v_3 w_1 \kappa \beta^* + 2v_3 w_2 \beta^*)(w_4 + w_5) < 0 \tag{42}$$

and again inserting (36), (38) and (41) in (34) we obtain the value of b as

$$b = v_3(\kappa x_1^0 + x_2^0)(w_4 + w_5) > 0. \tag{43}$$

Clearly, $a < 0$ since $w_1, w_2 < 0$ and the other components forming a are positive. Also, $b > 0$ because $v_3 > 0, (\kappa x_1^0 + x_2^0) > 0, (w_4 + w_5) > 0$. This observation shows that the model (2)–(7) undergoes forward bifurcation when $\mathscr{R}_0 = 1$. This means that the disease free equilibrium changes from stable to unstable and the endemic equilibrium point becomes locally asymptotically stable. This proves the local asymptotic stability of the EEP which was not clear.

4. Numerical Analysis of the Model

4.1. Parameterization of the Model. We parameterize the model (2)–(7) using the Maximum Likelihood Estimation algorithm implemented in fitR package. We adopt the public data for the daily COVID-19 positive cases as reported by the government of the Republic of South Africa since June 01, 2020 to September 08, 2020 [14]. The best fit of the model is depicted by **Figure 2**.

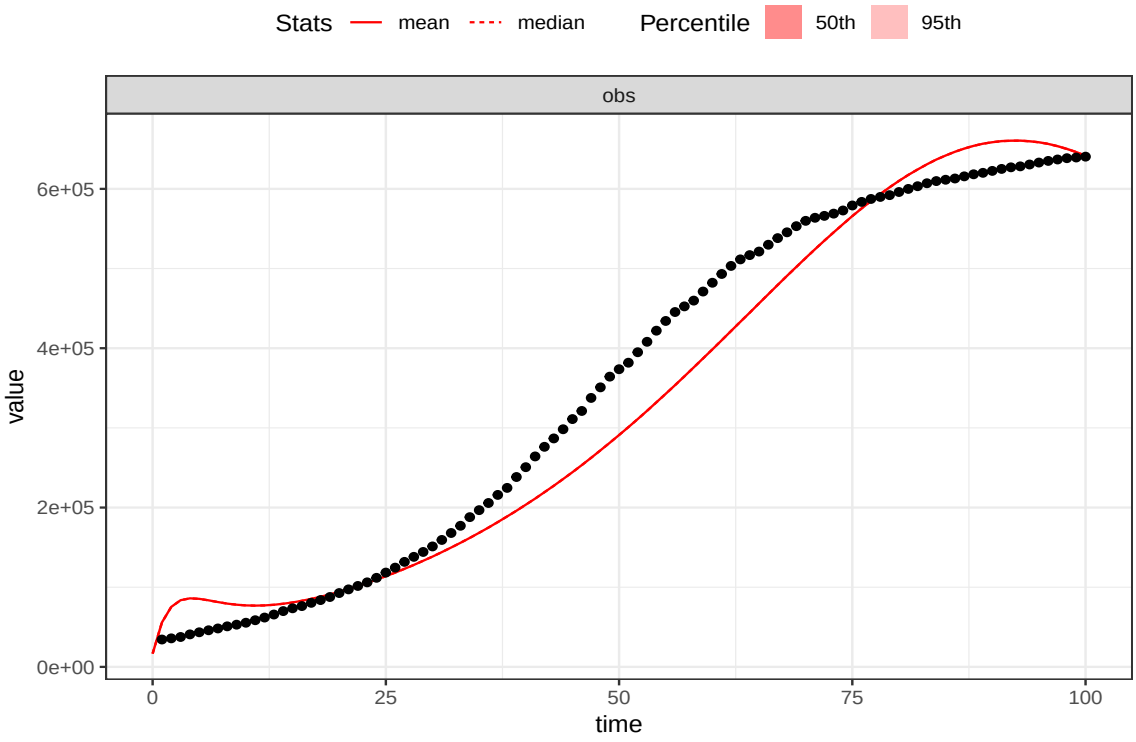

FIGURE 2. Fitting of the model (2)–(7) to COVID-19 positive reported cases (01 June - 08 September 2020) in the Republic of South Africa. The black-dotted line represents the reported data whereas the red-continuous line shows the model's best fit. Parameter values used are as listed in Table 1 where $\beta = 1.0598$ and $\rho = 0.46$.

4.2. Sensitivity Analysis. Generally, sensitivity analysis enables a researcher to ascertain the effect(s) of certain parameter(s) of research interest on the dependent variable [27]. For our model, we perform the sensitivity analysis to establish the effect(s) of the parameter β (denoting the contact rate of susceptibles with infectious individuals but measuring direct infection rate of individuals with comorbidity) and the parameter ρ (representing the proportion of infectious individuals with comorbidity), on the basic reproduction number $\mathscr{R}_0$. We find the partial derivatives of $\mathscr{R}_0$ with respect to β and ρ respectively and then find the sensitivity index for both parameters essentially for the sensitivity interpretation.

Differentiating equation (20) representing the basic reproduction partially with respect to β we have

$$\frac{\partial \mathscr{R}_0}{\partial \beta} = \pi\left(\frac{(1-\omega)\kappa}{\delta}+\frac{\omega}{\delta+\mu}\right)\left\{\frac{\rho\eta}{(\eta+\delta+\mu)(\psi+\delta+\mu)}+\frac{(1-\rho)\eta}{(\eta+\delta+\mu)(\alpha+\delta)}\right\}. \tag{44}$$

The sensitivity index of $\mathscr{R}_0$ with respect to β is

$$\mathscr{X}_{\beta}^{\mathscr{R}_0} = \frac{\partial \mathscr{R}_0}{\partial \beta}\times\frac{\beta}{\mathscr{R}_0} = 1. \tag{45}$$

Equation (45) hints that a unit change in β results to a proportional unit change in the $\mathscr{R}_0$. This means that for instance if β increases by 10%, then $\mathscr{R}_0$ also increases by 10% and if β decreases by 10%, then $\mathscr{R}_0$ also decreases by 10%. This unique trend is established in **Figure 3**.

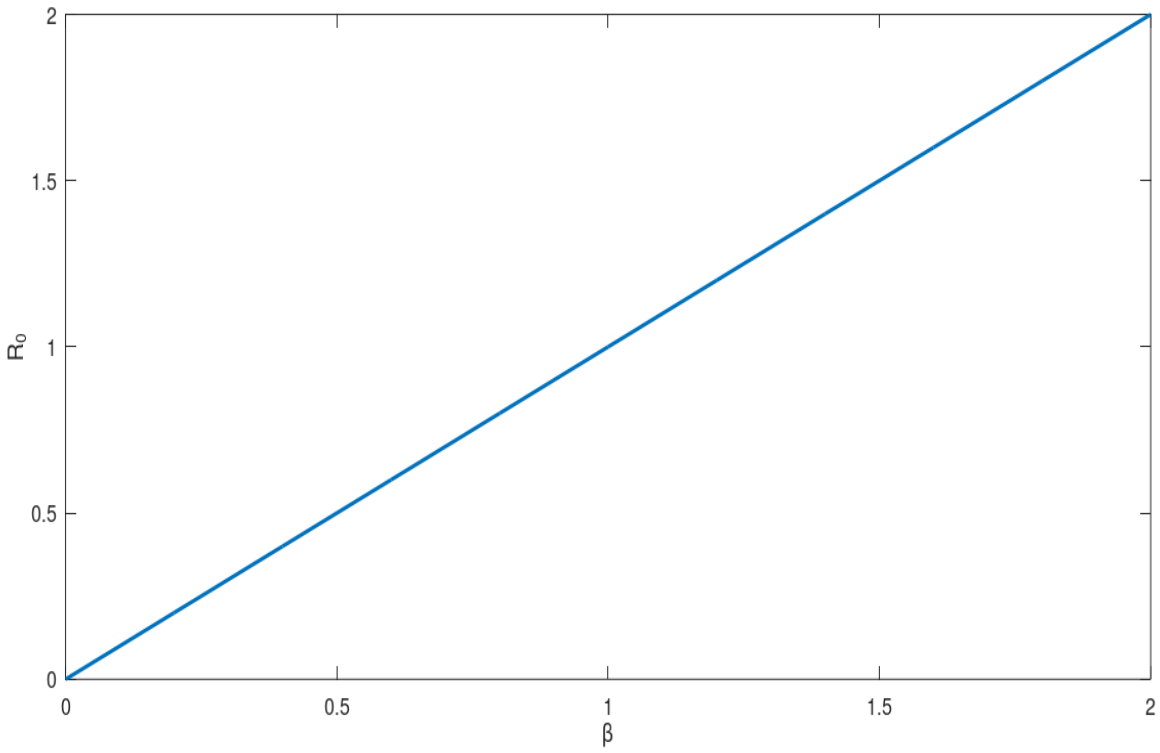

FIGURE 3. Sensitivity index of $\mathscr{R}_0$ with respect to β.

Similarly, differentiating equation (20) partially with respect to ρ we obtain

$$\frac{\partial \mathscr{R}_0}{\partial \rho} = \beta\pi\left(\frac{(1-\omega)\kappa}{\delta}+\frac{\omega}{\delta+\mu}\right)\left\{\frac{\eta}{(\eta+\delta+\mu)(\psi+\delta+\mu)}-\frac{\eta}{(\eta+\delta+\mu)(\alpha+\delta)}\right\}. \tag{46}$$

The sensitivity index of $\mathscr{R}_0$ with respect to ρ is

$$\mathscr{X}_{\rho}^{\mathscr{R}_0} = \frac{\partial \mathscr{R}_0}{\partial \rho}\times\frac{\rho}{\mathscr{R}_0} = \frac{1}{1+\frac{\psi+\delta+\mu}{(\alpha-\psi-\mu)\rho}}. \tag{47}$$

Equation (47) implies that a unit change in ρ results to a $\frac{1}{1+\frac{\psi+\delta+\mu}{(\alpha-\psi-\mu)\rho}}$ change in the $\mathscr{R}_0$. This observation is graphically interpreted by **Figure 4**. The figure reveals that an increase in ρ results to a gentle increase in $\mathscr{R}_0$ and vice versa. This observation gives an interpretation within the model that, if the proportion of the COVID-19 infectious individuals with comorbidity increases, then this also leads to increase in the value of the basic reproduction number which means more COVID-19 infections would be recorded.

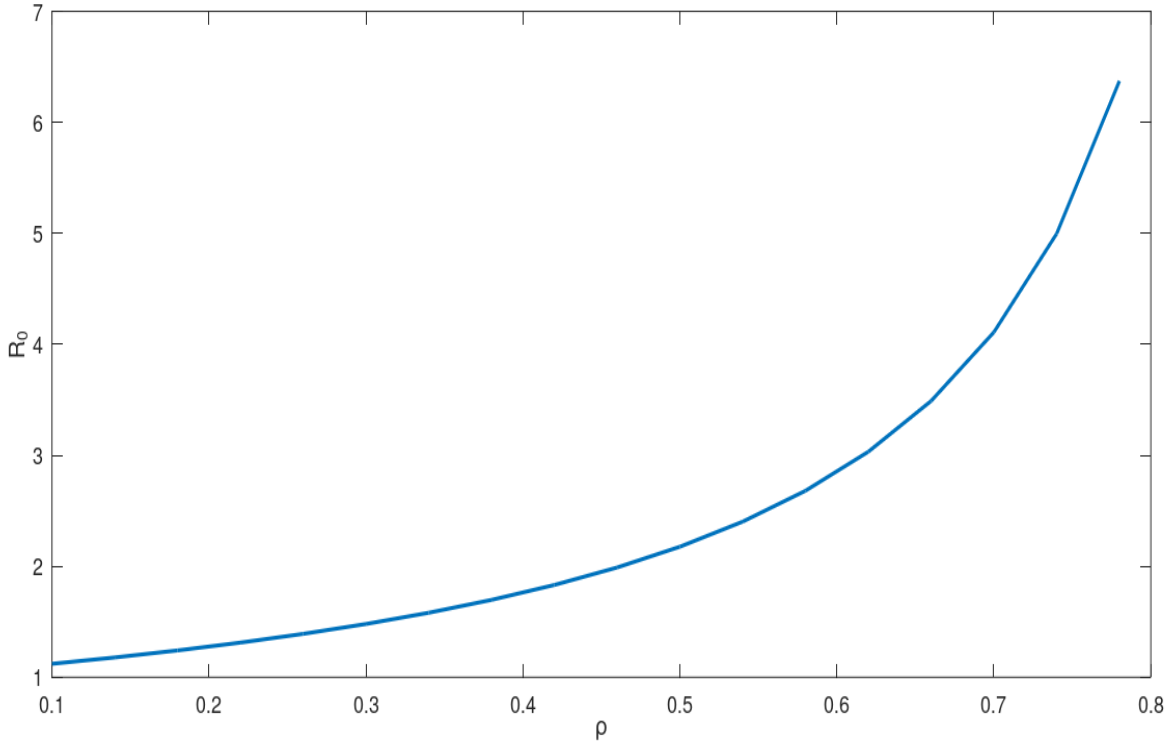

FIGURE 4. Sensitivity index of $\mathscr{R}_0$ with respect to ρ. Parameter values used are listed in Table 1.

4.3. Simulations. We carry out numerical simulations with respect to the parameters of interest using the calibrated model. The parameters of interest here for the proposed model are β and ρ. We vary these parameters and assess their impacts on the trajectory of the COVID-19 infections. The classes of the model adding up to the COVID-19 infections are the class of the COVID-19 infectious individuals with comorbidity I_c and the class of the COVID-19 infectious individuals without comorbidity I_0. We use parameter values listed in **Table 1**.

Figure 5 shows the trajectory of the COVID-19 infectious individuals with comorbidity I_c as β varies. We observe from the figure that as β increases, the number of the COVID-19 infectious individuals with comorbidity also increases but the infections take relatively shorter time to clear. Contrary, as β decreases, the number of the COVID-19 infectious individuals with comorbidity decreases but the infections delay to clear. This observation is explained by the fact that if individuals with comorbidity are highly exposed to the COVID-19 infections, then they highly contract the disease and hence rising the number of the COVID-19 infections. If their contact rate with the COVID-19 infectious individuals is reduced, then the infections reduce.

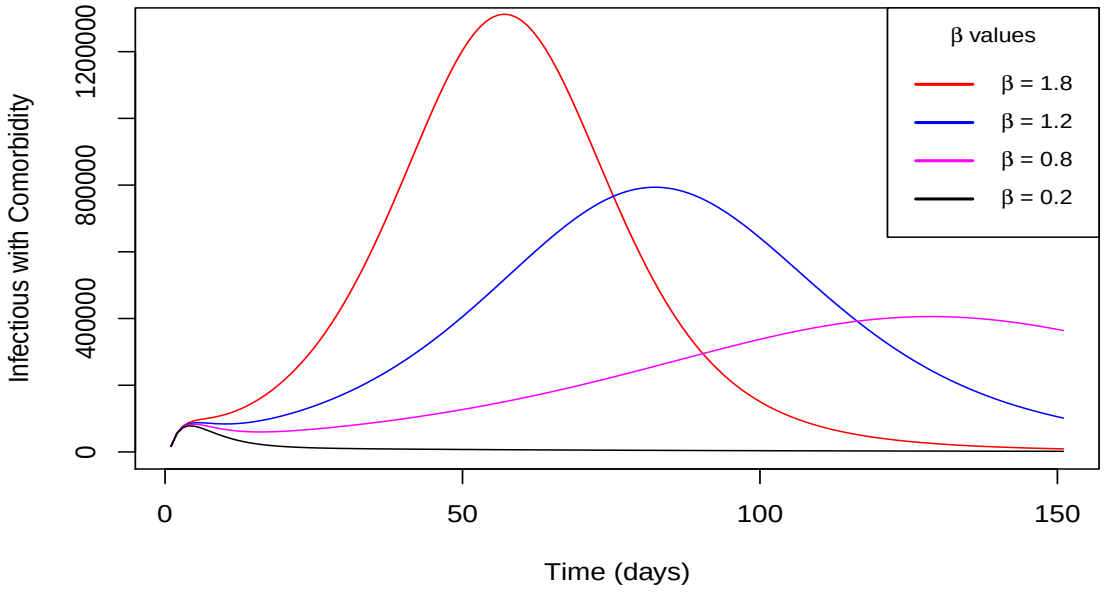

FIGURE 5. Trajectory of the COVID-19 infectious individuals with comorbidity I_c as β varies.

Figure 6 illustrates the trajectory of the COVID-19 infectious individuals with comorbidity I_c as ρ varies. We see from the figure that as ρ increases, the number of the COVID-19 infectious individuals with comorbidity also increases and the infections take relatively longer time to clear. On the other hand, as ρ decreases, the number of the COVID-19 infectious individuals with comorbidity highly reduces at an accelerated rate.

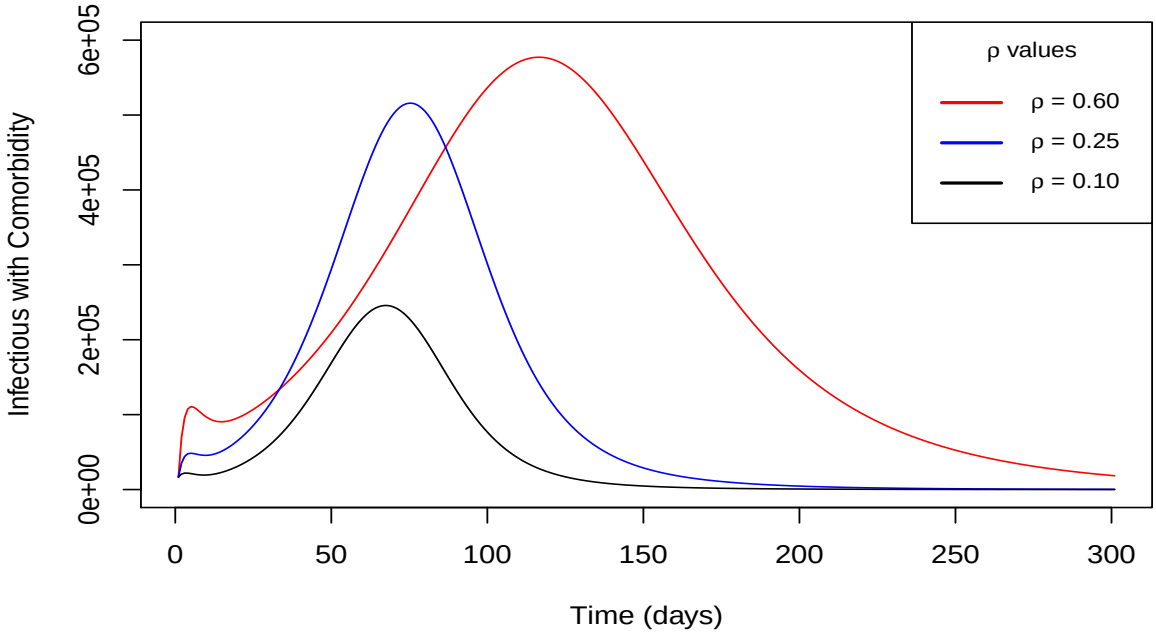

FIGURE 6. Trajectory of the COVID-19 infectious individuals with comorbidity I_c as ρ varies.

Figure 7 shows the trajectory of the COVID-19 infectious individuals without comorbidity I_0 as β changes. It is observable from the figure that as β increases, the number of the COVID-19 infectious individuals without comorbidity increases though the infections clear at an accelerated rate. Conversely, as β decreases, the number of the COVID-19 infectious individuals without comorbidity also decreases with the infections delaying to clear. This implies that increased contact rate with the COVID-19 infectious individuals will result to increased number of the COVID-19 infections recorded. This can be reversed by reducing the contact rate by imposing a control measure strategy to reduce the infections.

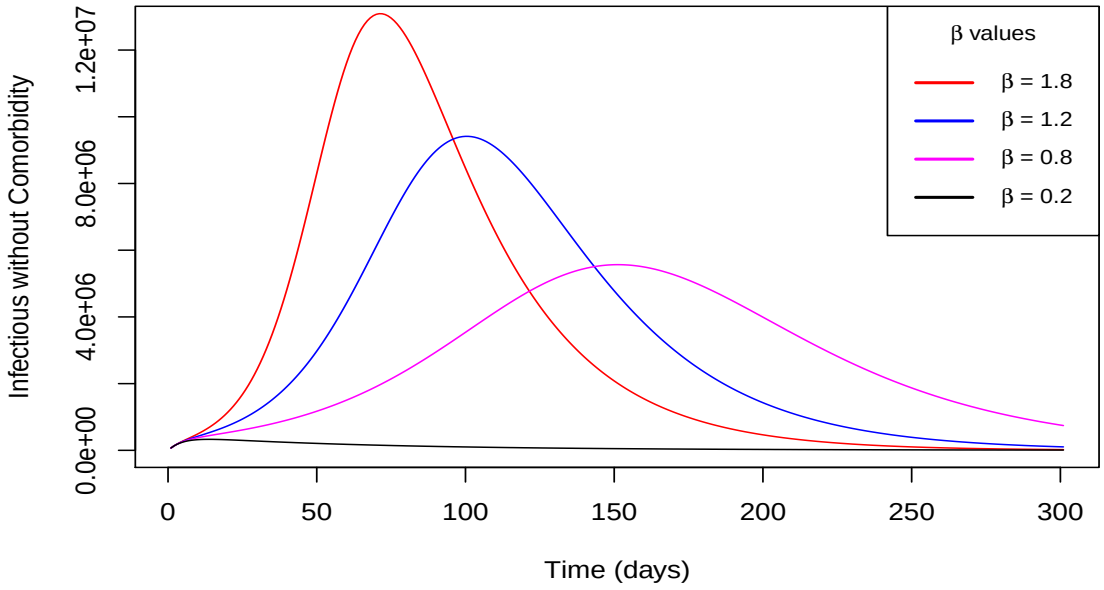

FIGURE 7. Trajectory of the COVID-19 infectious individuals without comorbidity I_0 as β changes.

Figure 8 shows the trajectory of the COVID-19 infectious individuals without comorbidity I_0 as ρ changes. We observe from the figure that as ρ increases, the number of the COVID-19 infectious individuals without comorbidity decreases but with the infections delaying to clear. Contrary, as ρ decreases, the number of the COVID-19 infectious individuals without comorbidity increases but the infections are accelerated to clear. This is because as the proportion of the COVID-19 infectious individuals with comorbidity increases, the proportion of the COVID-19 infectious individuals without comorbidity decreases and vice versa.

5. CONCLUSION

The main purpose of this study was to assess the role of comorbidity on the COVID-19 infections. To achieve this purpose, we extended the standard *SEIR* mathematical model by adding compartments for individuals with comorbidity. The newly developed model was confined to those comorbidities that are not infectious and thus the model assumed that there was no transmission of comorbidities from one individual to another within the compartments of the model.

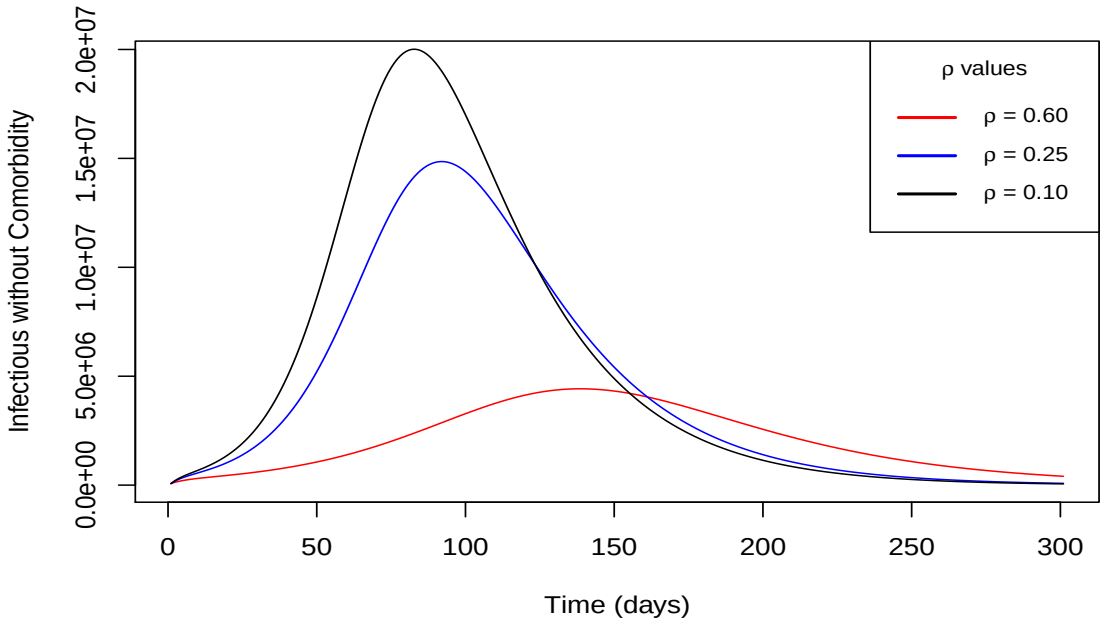

FIGURE 8. Trajectory of the COVID-19 infectious individuals without comorbidity I_0 as ρ changes.

We carried out the qualitative analysis of the model and ascertained that the solution of the model remained positive and bounded within a defined biological invariant region for all non-negative time. We further validated the model by fitting it to real data using the Maximum Likelihood Estimation algorithm implemented in fitR package. The data used here was the Republic of South Africa's COVID-19 positive cases reported data from June 01, 2020 to September 08, 2020. We next adopted the best fitted model to perform sensitivity analysis and numerical analysis.

For the sensitivity analysis, we used the expression for the basic reproduction number $\mathscr{R}_0$ to compute partial derivatives of $\mathscr{R}_0$ with respect to the parameters of interest β and ρ. We then found the sensitivity indices with respect to the aforementioned parameters of interest for the purpose of sensitivity interpretation. It was found that a unit change in β resulted to a proportional unit change in the $\mathscr{R}_0$. This meant that for example if β increased by 10%, then $\mathscr{R}_0$ would also increase by 10% and if β decreased by 10%, then $\mathscr{R}_0$ would also decrease by 10%. Similarly, we found that a unit change in ρ resulted to a $\frac{1}{1+\frac{\psi+\delta+\mu}{(\alpha-\psi-\mu)\rho}}$ change in the $\mathscr{R}_0$.

Graphical interpretation of this observation showed that an increase in ρ resulted to a gentle increase in $\mathscr{R}_0$ and vice versa.

For the numerical simulations, we varied β and ρ and observed their impacts on the number of COVID-19 infectious individuals with comorbidity and the number of COVID-19 infectious individuals without comorbidity. Results indicated that increase in β and ρ resulted to increase in the number of COVID-19 infectious individuals with comorbidity and vice versa. However, though increase in β resulted to increase in the number of COVID-19 infectious individuals without comorbidity, increase in ρ resulted to decrease in the number of COVID-19 infectious individuals without comorbidity.

ACKNOWLEDGMENTS

M. Kinyili and JMS. Lubuma acknowledges the South African National Research Foundation (NRF). M. Kinyili also acknowledges the University of the Witwatersrand and UWC.

CONFLICT OF INTERESTS

The authors declare that there is no conflict of interests.

REFERENCES

[1] S. M. Garba, J. M. Lubuma, and B. Tsanou, Modeling the transmission dynamics of the COVID-19 Pandemic in South Africa, Math. Biosci. 328 (2020), 108441.

[2] S. E. Eikenberry, M. Mancuso, E. Iboi, T. Phan, K. Eikenberry, Y. Kuang, E. Kostelich, A. B. Gumel, To mask or not to mask: Modeling the potential for face mask use by the general public to curtail the COVID-19 pandemic, Infect. Dis. Model. 5 (2020), 293–308.

[3] M. Kinyili and M. Wanyonyi, Forecasting of Covid-19 Deaths in South Africa Using Autoregressive Integrated Moving Average (ARIMA) Time Series Model, Gen. Lett. Math. 11 (2022), 26–35.

[4] Z. Mukandavire, F. Nyabadza, N. J. Malunguza, D. F. Cuadros, T. Shiri, and G. Musuka, Quantifying early COVID-19 outbreak transmission in South Africa and exploring vaccine efficacy scenarios, PloS One, 15 (2020), e0236003.

[5] M. Arashi, A. Bekker, M. Salehi, S. Millard, B. Erasmus, T. Cronje, and M. Golpaygani, Spatial analysis and prediction of COVID-19 spread in South Africa after lockdown, arXiv preprint arXiv, 2005 (2020), 09596.

[6] M. Kinyili, J.B. Munyakazi, A.Y.A. Mukhtar, Modeling the impact of combined use of covid alert SA app and vaccination to curb Covid-19 infections in South Africa, PLOS ONE 18 (2023), e0264863.

[7] A. Ishtiaq, Dynamics of COVID-19 Transmission: Compartmental-based mathematical modeling, Life Sci. 1 (2020), 5.

[8] S. B. Bastos and D. O. Cajueiro, Modeling and forecasting the early evolution of the Covid-19 pandemic in Brazil, Sci. Rep. 10 (2020), 1–10.

[9] M. Kinyili, J. B. Munyakazi and A. Y Mukhtar, To use face masks or not after COVID-19 vaccination? An impact analysis using mathematical modelling, Front. Appl. Math. Stat. 15 (2022), 872284.

[10] A. Mollalo, B. Vahedi, and K. M. Rivera, GIS-based spatial modeling of COVID-19 incidence rate in the continental United States, Sci. Total Environ. 728 (2020), 138884.

[11] A. Atangana and S. I. Araz, Mathematical model of COVID-19 spread in Turkey and South Africa: theory, methods, and applications, Adv. Differ. Equ 2020 (2020), 1–89.

[12] A. N. Góis, E. E. Laureano, D. D. Santos, et al. Lockdown as an intervention measure to mitigate the Spread of COVID-19: a modeling study, Revista da Sociedade Brasileira de Medicina Tropical, 53 (2020), e20200417.

[13] K. G. Mekonen, S. F. Balcha, L. L. Obsu, and A. Hassen, Mathematical Modeling and Analysis of TB and COVID-19 Coinfection, J. Appl. Math. 2022 (2022), 2449710.

[14] The Republic of South Africa's department of Health online resource and news portal on COVID-19, https://www.SAcoronavirus.co.za (2020).

[15] W. Bolin, R. Li, Z. Lu, and Y. Huang, Does comorbidity increase the risk of patients with COVID-19: evidence from meta-analysis, Aging 12 (2020), 6049.

[16] Z. Noémi, S. Váncsa, N. Farkas, P. Hegyi, and B. Eross, The negative impact of comorbidities on the disease course of COVID-19, Intensive Care Medicine, 46 (2020),1784–1786.

[17] Y. Chanyuan, S. Zhang, X. Zhang, H. Cai, J. Gu, J. Lian, Y. Lu et al, Impact of comorbidities on patients with COVID-19: a large retrospective study in Zhejiang, China, J. Med. Virol. 92 (2020), 2821–2829.

[18] A. K. Singh and A. Misra, Impact of COVID-19 and comorbidities on health and economics: Focus on developing countries and India, Diabetes Metab Syndr: Clin. Res. Rev. 14 (2020), 1625–1630.

[19] A. Sanyaolu, C. Okorie, A. Marinkovic, et al. Comorbidity and its impact on patients with COVID-19, SN Compr. Clin. Med. 2 (2020), 1069–1076.

[20] S. P. Dai, X. Zhao, and J. Wu, Effects of comorbidities on the elderly patients with COVID-19: clinical characteristics of elderly patients infected with COVID-19 from sichuan, China, J. Nutr. Health Aging, 25 (2021), 18–24.

[21] A. Gülsen, R. Inke R, U. Jappe, and D. Drömann, Effect of comorbid pulmonary disease on the severity of COVID-19: A systematic review and meta-analysis, Respirology, 26 (2021), 552–565.

[22] S. Jia, M. Zeng, H. Wang, C. Qin, H. Hou, Z. Sun, S. Xu et al, Distinct effects of asthma and COPD comorbidity on disease expression and outcome in patients with COVID-19, Allergy, 76 (2021), 483–496.

[23] B. K. Tsankov, M. Joannie, M. A. Allaire, A. Irvine, J. Laura, B. A. Vallance, and K. Jacobson, Severe COVID-19 infection and pediatric comorbidities: a systematic review and meta-analysis, Int. J. Infect. Dis. 103 (2021), 246–256.

[24] F. Nyabadza, F. Chirove, C. W. Chukwu, and M. V. Visaya, Modelling the potential impact of social distancing on the COVID-19 epidemic in South Africa, Comput. Math. Methods Med. 2020 (2020), 5379278.

[25] D. M. Kennedy, G. J. Zambrano, Y. Wang, and O. P. Neto, Modeling the effects of intervention strategies on COVID-19 transmission dynamics, J. Clin. Virol. 128 (2020), 104440.

[26] Q. Yang, C. Yi, A. Vajdi, L. W. Cohnstaedt, H. Wu, X. Guo, and C. M Scoglio, Short-term forecasts and long-term mitigation evaluations for the COVID-19 epidemic in Hubei Province, China, Infect. Dis. Model. 5 (2020), 563–74.

[27] M. Kinyili, J. B. Munyakazi, and A. Y. A. Mukhtar, Mathematical Modeling and Impact Analysis of the use of COVID Alert SA app, AIMS Public Health, 9 (2022), 106–128.

[28] W. Lyra, J. D. do Nascimento Jr, J. Belkhiria, et al. COVID-19 pandemics modeling with modified determinist SEIR, social distancing, and age stratification. The effect of vertical confinement and release in Brazil, Plos One, 15 (2020), e0237627.

[29] T. Li, Y. Liu, M. Li, X. Qian, and S. Y. Dai, Mask or no mask for COVID-19: A public health and market study, PloS One, 15 (2020), e0237691.

[30] J. Howard, A. Huang, Z. Li, et al. An evidence review of face masks against COVID-19, Proc. Nat. Acad. Sci. 118 (2021), e2014564118 .

[31] M. Shen, J. Zu, C. K. Fairley, et al. Effects of New York's executive order on face mask use on COVID-19 infections and mortality: A modeling study, J. Urban Health, 98 (2021), 197–204.

[32] D. M. Mason, M. Kapinaj, A. P. Martínez, and L. Stella, Impact of social distancing to mitigate the spread of COVID-19 in a virtual environment, in: Proceedings of the ACM Symposium on Virtual Reality Software and Technology, (2020), 1–3.

[33] R. O. Stutt, R. Retkute, M. Bradley, et al. Modelling framework to assess the likely effectiveness of face-masks in combination with 'lock-down' in managing the COVID-19 pandemic, Proc. R. Soc. A, 476 (2020), 20200376.

[34] S. Moore, E. M. Hill, M. J. Tildesley, L. Dyson, and M. J. Keeling, Vaccination and non-pharmaceutical interventions for COVID-19: a mathematical modelling study, Lancet Infect. Dis. 21 (2021), 793–802.

[35] S. M. Moghadas, T. N. Vilches, K. Zhang, et al. Evaluation of COVID-19 vaccination strategies with a delayed second dose, PLoS Biol. 19 (2021), e3001211.

[36] B. H. Foy, B. Wahl, K. Mehta, et al. Comparing COVID-19 vaccine allocation strategies in India: A mathematical modelling study, Int. J. Infect. Dis 103 (2021), 431–438.

[37] A. Olivares and E. Staffetti, Uncertainty quantification of a mathematical model of COVID-19 transmission dynamics with mass vaccination strategy, Chaos Solitons Fractals, 146 (2021), 110895.

[38] M. Sadarangani, B. A Raya, J. M. Conway, et al. Importance of COVID-19 vaccine efficacy in older age groups, Vaccine, 39 (2021), 2020–2023.

[39] M. Kinyili, J. B. Munyakazi, and A. Y. A. Mukhtar, Assessing the impact of vaccination on COVID-19 in South Africa using mathematical modeling, Appl. Math. Inf. Sci. 15 (2021), 701–716.

[40] E. A. Iboi, C. N. Ngonghala, and A. B. Gumel, Will an imperfect vaccine curtail the COVID-19 pandemic in the US?, Infect. Dis. Model. 5 (2020), 510–24.

[41] A. B. Gumel, E. A. Iboi, C. N. Ngonghala, and G. A. Ngwa, Mathematical assessment of the roles of vaccination and non-pharmaceutical interventions on COVID-19 dynamics: a multigroup modeling approach, medRxiv, (2021), 2020–12.

[42] S. Anusha, and S. Athithan, Mathematical modelling co-existence of diabetes and COVID-19: Deterministic and stochastic approach, (2021). https://doi.org/10.21203/rs.3.rs-862792/v1.

[43] P. Das, R. K, Upadhyay, A. K. Misra, A. R. Fathalla, D. Pritha, and D. Ghosh, Mathematical model of COVID-19 with comorbidity and controlling using non-pharmaceutical interventions and vaccination, Nonlinear Dyn. 106 (2021), 1213–1227.

[44] A. Kouidere, E. Y. Lahcen, H. Ferjouchia, O. Balatif, and M. Rachik, Optimal Control of Mathematical modeling of the spread of the COVID-19 pandemic with highlighting the negative impact of quarantine on diabetics people with Cost-effectiveness, Chaos Solitons Fractals, 145 (2021), 110777.

[45] C. Castillo-Chavez, B. Song, and W. Huang, On the computation of R_0 and its role in global stability, IMA Vol. Math. Appl. 125 (2002), 229–50.

[46] C. Castillo-Chavez, and B. Song, Dynamical models of tuberculosis and their applications, Math. Biosci. Eng. 1 (2004), 361.

[47] G. G. Muthuri, D. M. Malonza, and F. Nyabadza, Modeling the effects of treatment on alcohol abuse in Kenya incorporating mass media campaign, J. Math. Comput. Sci. 9 (2019), 632–653.